

Signal and background studies for ECN3

Iaroslava Bezshyiko, Oliver Lantwin, Maksym Ovchynnikov, Anupama Reghunath

October 1, 2024

Abstract

In this report, we summarize physics studies performed for the SHiP experiment: neutrino deep-inelastic scattering background, muon deep-inelastic scattering background, and sensitivity to new physics particles. The report contains research work carried out up to summer 2024. Namely, we recapitulate the main steps of the analysis that appeared in the SHiP LoI to make them reproducible. We also highlight features to be improved in future studies.

Contents

1 Neutrino DIS	2
1.1 Core concepts	2
1.2 Neutrino simulation	2
1.3 Candidate signature	5
1.4 Neutrino estimations	6
1.4.1 CDS studies	6
1.4.2 ECN3 studies	9
2 Muon DIS	14
2.1 Simulation details	14
2.2 front and side muons	15
2.3 Cavern muons	21
3 Sensitivities to feebly-interacting particles	22
3.1 Future plans	25
4 Muon combinatorial	26
A Appendix	27

1 Neutrino DIS

Iaroslava Bezshyiko

1.1 Core concepts

The danger of the neutrino-induced background for the SHiP experiment is that this background itself is dominated by decays of long-lived neutral SM particles decaying within the decay volume due to inelastic neutrino scattering. The difficulty is that these particles can decay to the same final states as the new physics (NP) particles and we cannot see with any detection system that a neutrino has entered the decay volume.

The schematic idea that illustrates why neutrinos are fatal for us is shown in Figure 1. Most neutrinos are created immediately after the proton-nuclei collision in the target. As they only interact weakly, almost all of them reach the decay volume without being influenced by the hadron absorber or muon shield. Since they are neutral, they may enter the fiducial volume without being detected by upstream and surrounding veto systems. There they can interact inelastically in the vicinity of the decay volume and produce short- and long-lived neutral particles that can fly on and completely mimic the signal decay in the spectrometer. It is crucial for the experiment to be able to exclude such background events based solely on their topological difference compared to the signal events. The strategy for this is to generate a sufficiently large Monte Carlo sample to study the kinematic properties of the neutrinos.

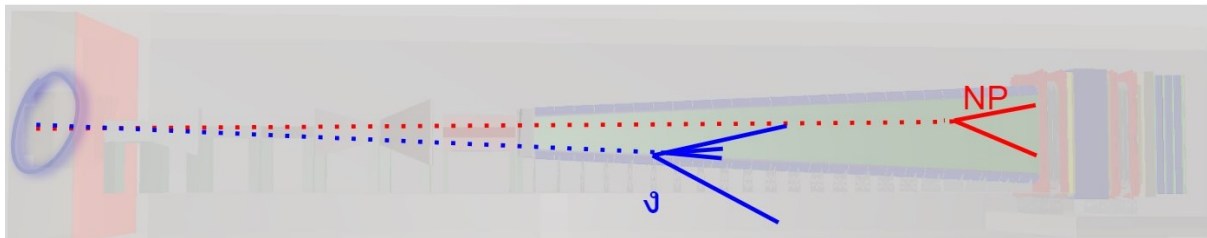


Figure 1: An illustrative comparison of the neutrino-induced background in the decay volume. The neutrino generated in the target (blue) reaches the decay volume and interacts inelastically with the material of the decay vessel. The newly produced particles can then reach the straw tracker and mimic the signal vertex (in red) within the fiducial volume.

1.2 Neutrino simulation

The entire simulation of the experiment is done in the FairRoot framework, in which the interaction of particles with matter is implemented with GEANT4. However, it is known that GEANT4 cannot simulate the spectrum of charm mesons accurately enough. Additionally, the initial proton-proton collision step is extremely time-consuming and computationally expensive. For this reason, the initial proton-target collision is performed in the `pythia8` generator and the results are transferred to GEANT4 to simulate the detector response. The subtlety is that, until recently, GEANT4 was not able to simulate neutrino interactions. For this reason, the GENIE software is used to simulate the neutrino charge-current and neutral-current interactions with the detector material. Only then are the interaction products further processed by GEANT4. The entire neutrino simulation process can therefore be divided into four steps:

1. The simulation of proton-on-target (POT) interactions with `pythia8` and the extraction of a momentum distribution of the produced neutrinos. The momentum distributions

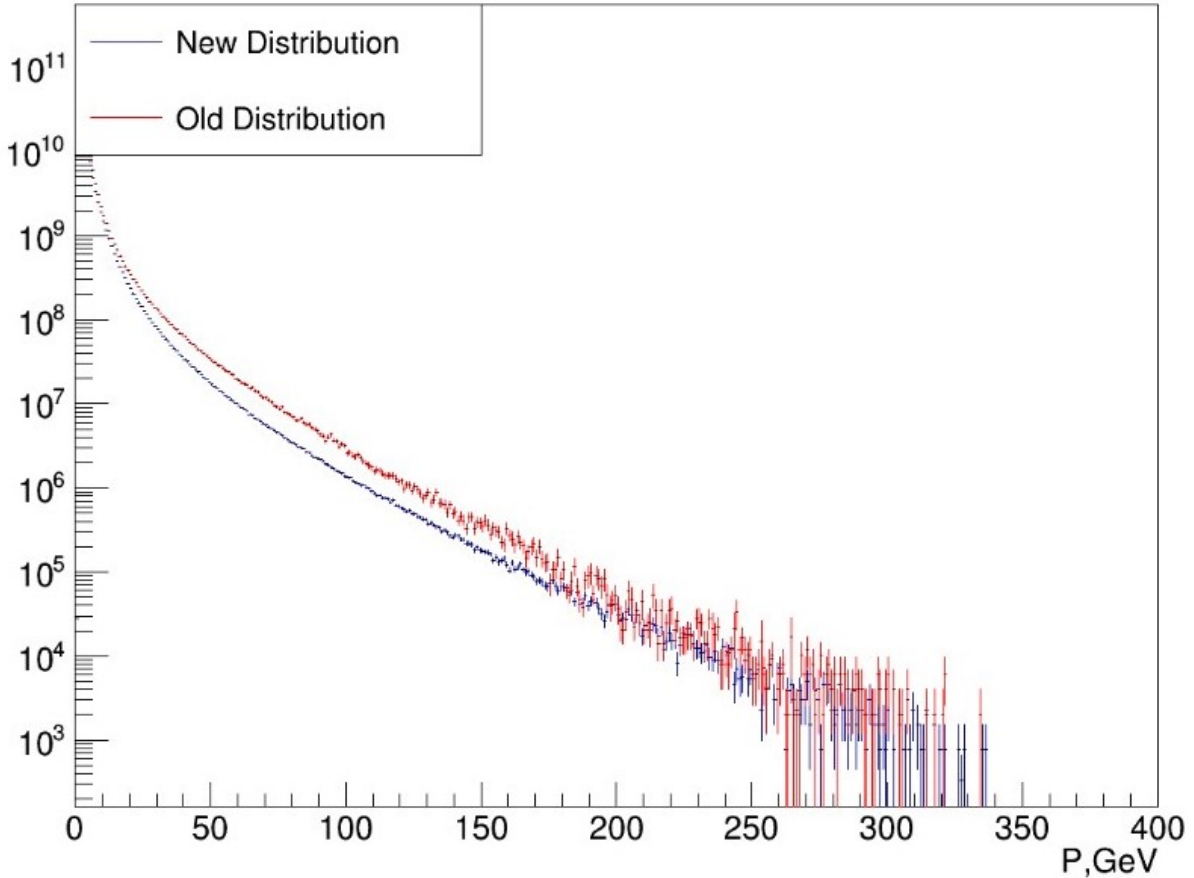


Figure 2: Momentum distribution of muon neutrino out of `pythia8` POT simulation. Old distribution corresponds to the POT simulations done for the Technical Proposal; new simulations correspond to POT simulations done in 2018 and have higher statistic and more data with two energy cuts of 1 GeV and 10 GeV, and also includes heavy-flavour cascade production in the target

for two different POT generations for muon neutrinos is shown in Figure 2. The “old distribution” in the plot corresponds to the one of the first POT generations done for the technical proposal (TP) studies (2014–2015). The “new distribution” corresponds to the bigger POT generation done in 2018, including two separate productions with energy cuts of 10 GeV and 1 GeV, and also includes heavy-flavour cascade production in the target [1]. The description of how the fixed-target generation is done in SHiP can be found in [2]

2. The obtained spectrum of neutrinos is given afterwards to GENIE to generate neutrino interactions with material.
3. As output of GENIE we have a set of particles produced in interactions which we pass to GEANT4. We place our particles in z -region between SND and second tracking station to maximise the statistics in the area of interest.
4. Using a P/P_T distribution we position our event in the geometry based on its weight. The weight of the event is given by $\sum \rho \cdot l$, where ρ is the density of the material which neutrino path and l is the distance. It is important to consider events only with their weights, as it

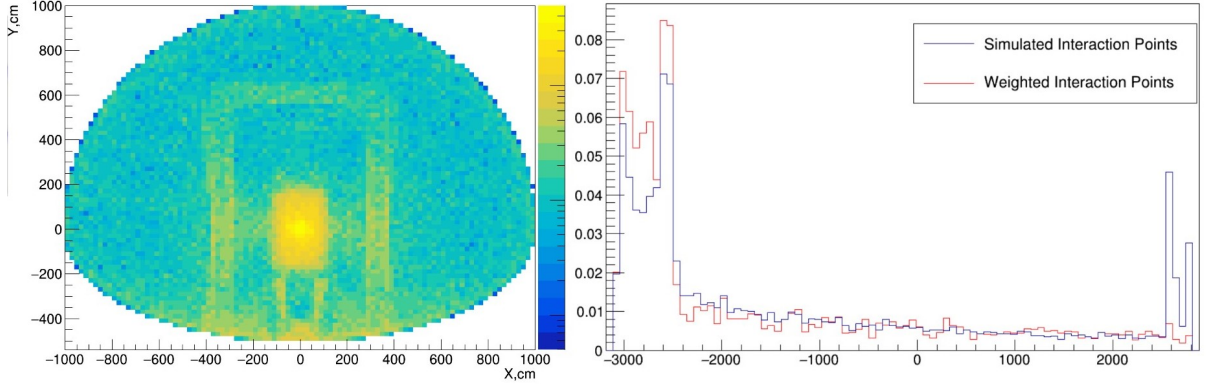


Figure 3: The spatial position of the neutrino interaction points in x - y (left) and z (right). The events are weighted in the left-hand diagram. One can see the material density in space based on the number of expected neutrino interactions. In the right plot, the comparison between weighted and unweighted distributions is shown, emphasising the need to use only weighted events. The blue peak at the end isn't present in the red plot because all neutrinos of all trajectories are forced to interact. However, the amount of material is different for the different trajectories. Assuming infinite statistics, the distributions of weighted and unweighted events coincide.

represents the probability for the neutrino to interact. An example of neutrino interactions location is shown in Figure 3.

After completing this procedure, we are left with simulated neutrino interactions as a function of the material density and the momentum distribution in the fiducial volume, which we can study. But what we really want to know is how many neutrino interactions we will have in the years that the experiment runs, where 5 years were considered for this study. The important fact that emerges from the simulation procedure is that different simulated events will have different actual values if you do the calculation for 5 years. To recalculate the number of neutrino interactions in 5 years, we need to add up all the events:

$$N_{\text{interactions}} = \sum \text{weight}_i$$

,where

$$\text{weight}_i = \frac{\rho_i \cdot L_i \cdot N_A \cdot N_\nu \cdot \sigma_i}{N_{\text{generated}}}$$

The weight of the event which we have from simulation: $w_i = \rho_i \cdot L_i$. Therefore, we can rewrite our equation:

$$\text{weight}_i = \sum \frac{w_i \cdot N_A \cdot N_\nu \cdot \frac{\sigma_i}{\text{GeV}} \cdot \langle E \rangle}{N_{\text{generated}}}$$

Here,

- $N_A = 6.022 \cdot 10^{23}$ — Avogadro constant.
- $N_{\text{generated}} = 1.5 \cdot 10^8$ — Number of simulated interactions.
- $N_\nu = 4.51 \cdot 10^{11} \cdot \frac{2 \cdot 10^{20}}{5 \cdot 10^{13}}$ — Number of expected neutrinos in 5 years taken from the `pythia8` simulation.
- $\frac{\sigma_i}{\text{GeV}} = 7 \cdot 10^{-39} \frac{\text{cm}^2}{\text{GeV}}$ — Neutrino cross-section taken from the Particle Data Group.

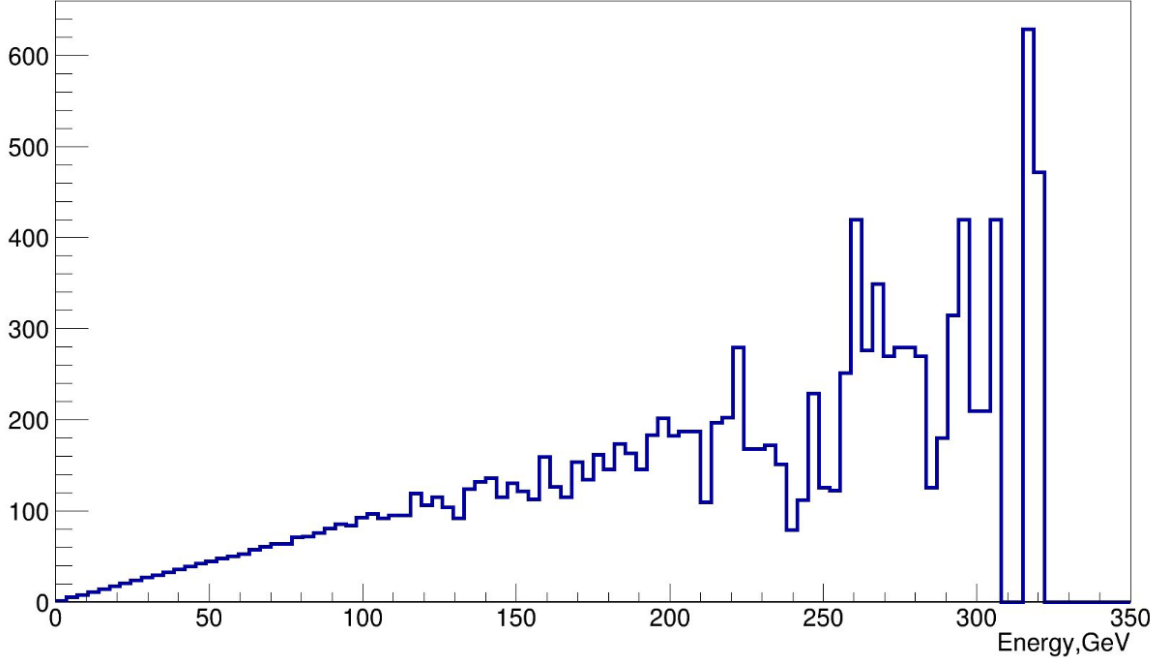


Figure 4: Ratio of the neutrino energy distribution from `pythia8` to the neutrino energy distribution from GENIE for simulations from 2016

- $\langle E \rangle = 2.57$ GeV — The average neutrino energy taken from the `pythia8` simulation.

It is important to use a neutrino energy because the neutrino cross section is energy dependent. We choose to use the average energy of the whole spectrum, since GENIE has a total neutrino cross section that depends linearly on the energy. This means that the ratio of the neutrino spectrum at generation and after interaction is a straight line. The plot in Fig. 4 shows the ratio of the neutrino energy distribution from `pythia8` to the neutrino energy distribution from GENIE for simulations from 2016.

1.3 Candidate signature

The common signature for all benchmark hidden sector (HS) models is an isolated vertex in the decay volume. Therefore, HS signal candidates are required to form an isolated vertex in the fiducial volume. All decay models can be also split in two categories: one which are fully reconstructed, meaning that all daughters coming from HS particle decay are reconstructible in the spectrometer and partially reconstructed, meaning that one or more daughters that come from HS particle decay cannot be reconstructed in the spectrometer (for instance, neutrinos). One of the strongest requirement for the signal selection is that an event must point back to the target, therefore its impact parameter must be less than 10 cm. Unfortunately, while this selection works great for the fully reconstructed events, partially reconstructed final states are more challenging to discriminate. Due to the fact that we are missing some particles, reconstructed event will point more loosely to the target. In this case, the signal candidates are required to have an impact parameter less than 250 cm. To separate them better we also require to have no activity in the surrounding the decay volume detectors. Selection on the track and vertex quality, as well as on the distance from the material is also applied.

1.4 Neutrino estimations

1.4.1 CDS studies

Several studies to understand the neutrino induced background have been performed for the CDS.

1. The estimation of neutrino-induced background events coming directly from the vicinity of the decay volume when the decay volume is kept under the atmospheric pressure. These studies were performed with an old geometry in which the decay volume has a cylindrical shape. The selection established at that time made it possible to achieve 1.56 fully reconstructed neutrino events and 30 partially reconstructed events. The results of these studies led to a relaxation of the vacuum requirements from 0.01 mbar to 1 mbar.
2. It was verified that neither of the two tracks reconstructed in the tracker, which form a loose vertex, were produced by the neutrino interaction in the cavern walls. Since these interactions do not produce a background, the cavern walls were excluded from the interaction region in the simulations.
3. The large simulation sample was generated with neutrino interactions forced within the region of the decay volume. The region in z was defined as 5 m before the entrance of the decay volume and after the second tracking station. The number of neutrino interactions generated is $1.5 \cdot 10^8$.

This large sample was then used to understand the neutrino-induced background. Using the formula from the previous chapter, the number of neutrino interactions in 5 years of runtime was estimated to be $2.2 \cdot 10^7$ which is seven times larger than the generated number of events.

The expected number of signal candidates before selection is $6.5 \cdot 10^4$. We consider the candidates as signal events if we can construct a vertex within the fiducial volume which is made of two charged tracks. Most of these signal candidates are produced in the SND detector, in the entrance window and in the wall elements of the decay volume, so that a large fraction of the candidates can be rejected with veto systems. Candidates produced by neutrino interactions do not show good reconstruction quality. The selection based on the requirement that the distance of closest approach (DOCA) must be less than 1 cm and pointing towards a target with an impact parameter (IP) of less than 2.5 m results in the background level being less than one neutrino-induced candidate and 65% of signal events are preserved. If we tighten the impact parameter cut to a value of 1 m, we can maintain this performance without using the veto tagger information around the decay volume. The background cannot be kept at the same level if only the kinematic topology is used without tagger information for $IP < 2.5$ m. However, the reconstructed vertices of the remaining candidates tend to stay close to the walls of the decay volume because they are caused by short-lived particles originating from neutrino interactions within the walls. Vertices far from the walls are formed by long-lived particles with a high multiplicity. Therefore, we can keep the background level under control by making an additional selection based on the position of the reconstructed vertices within the decay volume. The correlation between the z position of the closest hit in SBT and the z position of the reconstructed vertex is shown in Figure 5. Therefore, we can get rid of these events by not requesting activity in anywhere SBT, but only around the position of the vertex.

The basic selection is defined based on the kinematic topology of events and the reconstruction quality of tracks and vertices and consists of:

- Only one reconstructed candidate per event.
- The reconstructed vertex is located within the fiducial volume of the decay vessel.

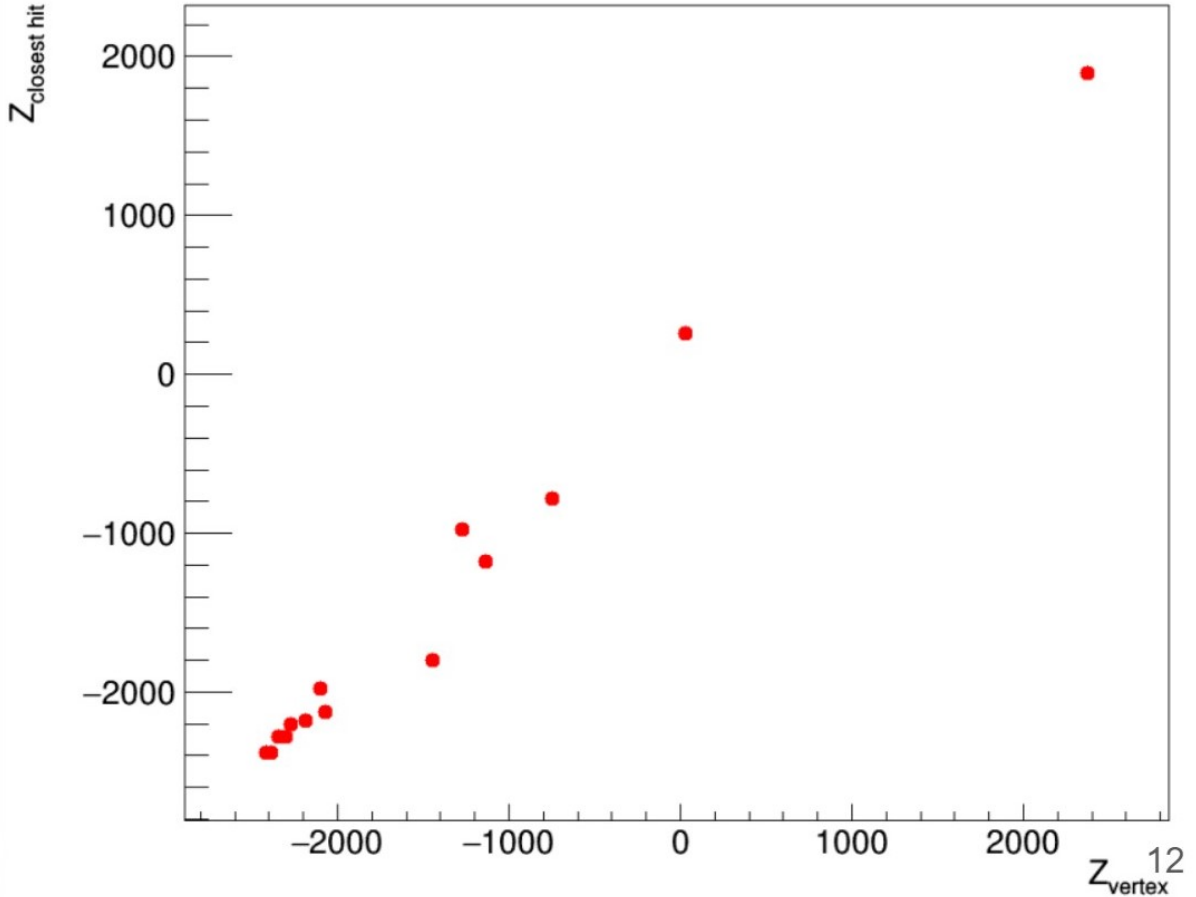


Figure 5: The correlation between the z position of the closest hit in the SBT and z position of the reconstructed vertex.

- The track fit converges for both daughters of the candidate and both tracks cross all four tracking stations.
- Number of degrees of freedom for tracks must be more than 25.
- DOCA between two charged tracks combining the vertex must be less than 1 cm.
- The reduced χ^2 of the track fit must be less than 5 for both daughters.
- The momentum of the daughter track must be greater than $1 \text{ GeV}/c$.
- Impact parameter to the target must be less than 10 cm for fully reconstructed events, and less than 2.5 m for partially reconstructed final states.

The rest of the background events consist of the event type shown in Figure 6, i.e. photon conversions in the material. They can be easily eliminated by requiring an invariant mass of the pair greater than $100 \text{ MeV}/c^2$. The only remaining background is caused by misidentification of particles and depends on the efficiency of the particle identification system. Nevertheless, these studies have shown that we can keep the background at a level of less than 0.1 events. The summary of the suppression level of the different selection criteria is shown in Table 1.

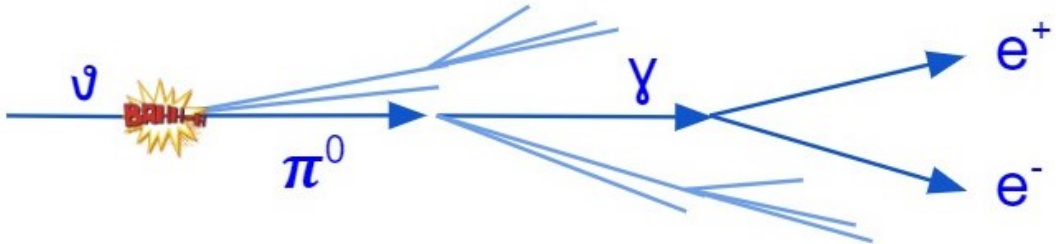
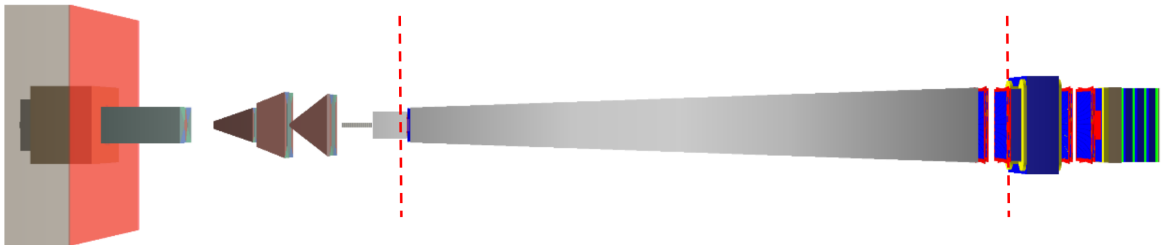


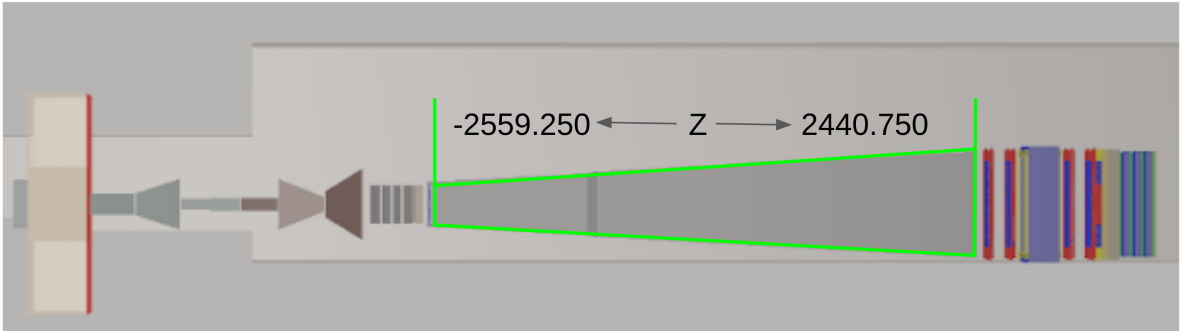
Figure 6: One type of neutrino-induced background events which are not affected by the basic selection and the requirement of no activity in the SBT around the vertex are photon conversions in the material. They can be easily eliminated by requiring an invariant mass of the pair of more than $100 \text{ MeV}/c^2$.

Selection Stage	$N_{\text{candidates}}$
Reconstructed candidates	65 612
Basic selection	135
PID	12
Exclude area next to material	8
Invariant mass $> 100 \text{ MeV}/c^2$	0.25
SBT signal around the vertex	0.05

Table 1: The table shows the suppression possibilities of the selection on the neutrino-induced background. Each row in the table corresponds to the sequential application of the cut to all previous ones. $N_{\text{candidates}}$ corresponds to the number of signal candidates from the neutrino-induced background in 5 years.



(a) The ECN3 geometry used for the simulation of the large sample. The red lines indicate the region in z where neutrino interactions were forced.



(b) The ECN3 geometry used for the simulation with a decay volume kept at atmospheric pressure. The green lines encapsulate the region where the neutrino interactions were forced.

Figure 7: Geometries used for simulations for the neutrino induced background studies at ECN3.

1.4.2 ECN3 studies

Following the decision to move the experiment to the ECN3 site, the neutrino background studies were updated to ensure that the geometry changes caused by the move to the new site would not result in significant changes to the background rates. Two types of studies were done:

1. A large simulation sample was generated with neutrino interactions forced in the region of the decay volume. The region in z was defined as 5 m before the entrance of the decay volume and after the second tracking station. The region for the neutrino interactions in the $x-y$ plane was not constrained, but the cavern walls were removed from the simulations to speed them up, as we have demonstrated that no candidates are formed from interactions in the cavern walls. The geometry that was used for this simulation is depicted in Figure 7a.
2. A simulation of neutrino interactions constrained within the decay volume when the decay volume is kept under atmospheric pressure. This simulation allows evaluating how many more neutrino induced background signal candidates will be produced in case the decay volume won't be kept under the vacuum. The geometry that was used for this simulation is depicted in Figure 7b.

A difference in the area of the muon shield and the SND detector can be observed for two geometries. This is due to historical reasons. The very first study performed, which isn't discussed in this report, was to check with the relatively small simulation sample that there are no obvious differences in the neutrino-induced background after optimising the experiment for the new location. Once this was confirmed, atmospheric pressure studies were performed

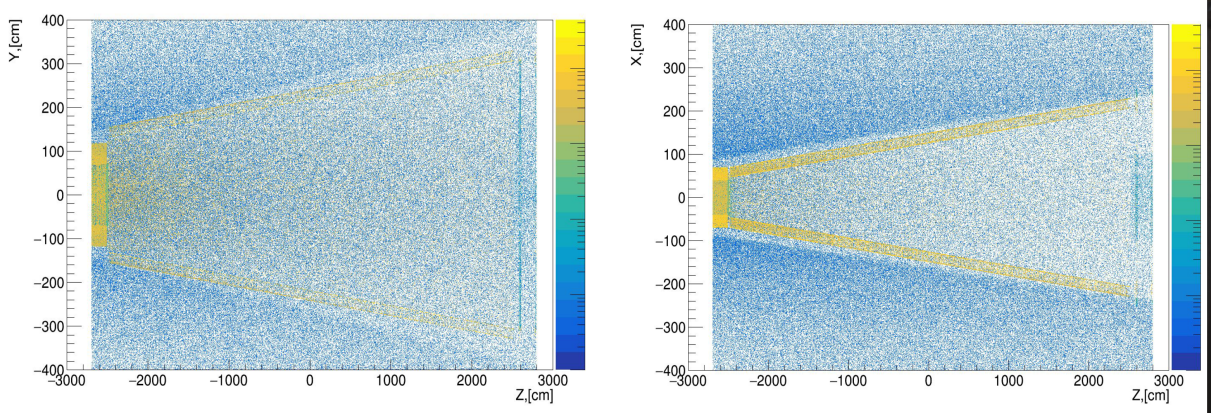


Figure 8: An example of neutrino interaction points in the simulated geometry. 10^6 events were used for the visualisation.

with the same geometry. At this point, all systems of ECN4 had merely been adjusted to the new sizes for ECN3, and the SND detector was replaced by tungsten blocks while further optimizations were performed. The large statistical studies were carried out later in the year 2023 when new versions of the muon shield and SND were introduced.

The large simulation sample $1.2 \cdot 10^8$ neutrino interactions were generated for the large statistical sample. After the reconstruction procedure, $5.3 \cdot 10^5$ reconstructed, generated signal candidates remained from the sample. An example of the positions of the neutrino interactions is shown in Figure 8. Only 10^6 neutrino interactions were used for the visualisation. The figure not only illustrates the shape of the different parts of the experiment due to the fact that the number of neutrino interactions depends on the density of the traversed material, but also shows the peculiarity resulting from the way the simulations are performed. It can be seen that the interactions in air aren't evenly distributed. This is explained by the fact that the neutrinos are distributed in the geometry according to the material density. Since we limit the region in z in which we force neutrinos from the entire P_T/P_z spectrum to interact, some neutrinos will only come into contact with air along their trajectory, while others will have to pass through more dense material. As the statistics increase, the visual effect disappears and the weighted events become more and more consistent with a real expected event. This emphasises the need to use only weighted neutrino interactions.

The result of the conversion of the generated events and signal candidates into the number of expected neutrinos is summarised in Table 2. While the number of neutrino interactions produced exceeds the expected number of neutrino interactions in five years by an order of magnitude, the number of reconstructed candidates produced from the neutrino-induced background exceeds the number of expected signal candidates from the neutrino-induced background by a factor of twenty. This indicates that we have even higher statistics in the region that produces more background candidates, which is due to the way the simulation is performed.

The basic selection for these samples was defined as followed:

- Only one reconstructed candidate per event.
- The reconstructed vertex is located within the fiducial volume of the decay vessel.
- The track fit converges for both daughters of the candidate and both tracks cross all four tracking stations.

	Generated events	Expected in 5 years
Number of neutrino interactions	$1.2 \cdot 10^8$	$1.2 \cdot 10^7$
Number of signal candidates	$5.3 \cdot 10^5$	$2.1 \cdot 10^4$

Table 2: The table shows the number of generated and expected neutrino induced events.

		Generated events	Expected in 5 years
Fully reconstructed events (IP < 10 cm)	Basic selection	10	0.06
	Basic selection and SBT	7	0.04
Partially reconstructed events (IP < 250 cm)	Basic selection	31	0.18
	Basic selection and SBT	1	0.006

Table 3: The table shows the number of generated and expected neutrino induced events after the selection for the large generated sample.

- Number of degrees of freedom for tracks must be more than 25.
- DOCA between two charged tracks combining the vertex must be less than 1 cm.
- The reduced χ^2 of the track fit must be less than 5 for both daughters.
- The momentum of the daughter track must be greater than 1 GeV.
- Impact parameter to the target must be less than 10 cm for fully reconstructed events, and less than 2.5 m for partially reconstructed final states.
- The reconstructed vertex should be at least 5 cm away from the walls of the decay volume.
- The reconstructed vertex should be 100 cm away from the entrance of the decay volume.
- There must be no response in the upstream veto detector.
- The particle identification system should define the two candidate tracks as hadron and lepton for events with impact parameter of less than 10 cm and as two leptons for events with impact parameter of less than 250 cm.

The results of applying this basic selection are shown in Table 3.

The simulation sample with decay volume kept under the atmospheric pressure. $1.6 \cdot 10^6$ neutrino interactions were generated within the decay volume when the decay volume is kept under atmospheric pressure. After the reconstruction procedure, 25 100 reconstructed generated signal candidates remained from the sample. These generated signal candidates yielded 1840 neutrino-induced signal candidates in five years of running after the conversion.

The simple check was also carried out to ensure that the simulations were implemented correctly and that the interactions really only take place in the air. Since we know that the weight of the event in the simulations is $\text{weight}_{\text{FairShip}} = \rho \cdot L$, where $\rho = 0.001205 \text{ g/cm}^3$ and $L = 5064 \text{ cm}$ we can estimate that $\text{weight}_{\text{FairShip}} \leq 6.1$ and therefore no events with higher weights should be present in the simulated sample. Figure 9 shows the distribution of weights

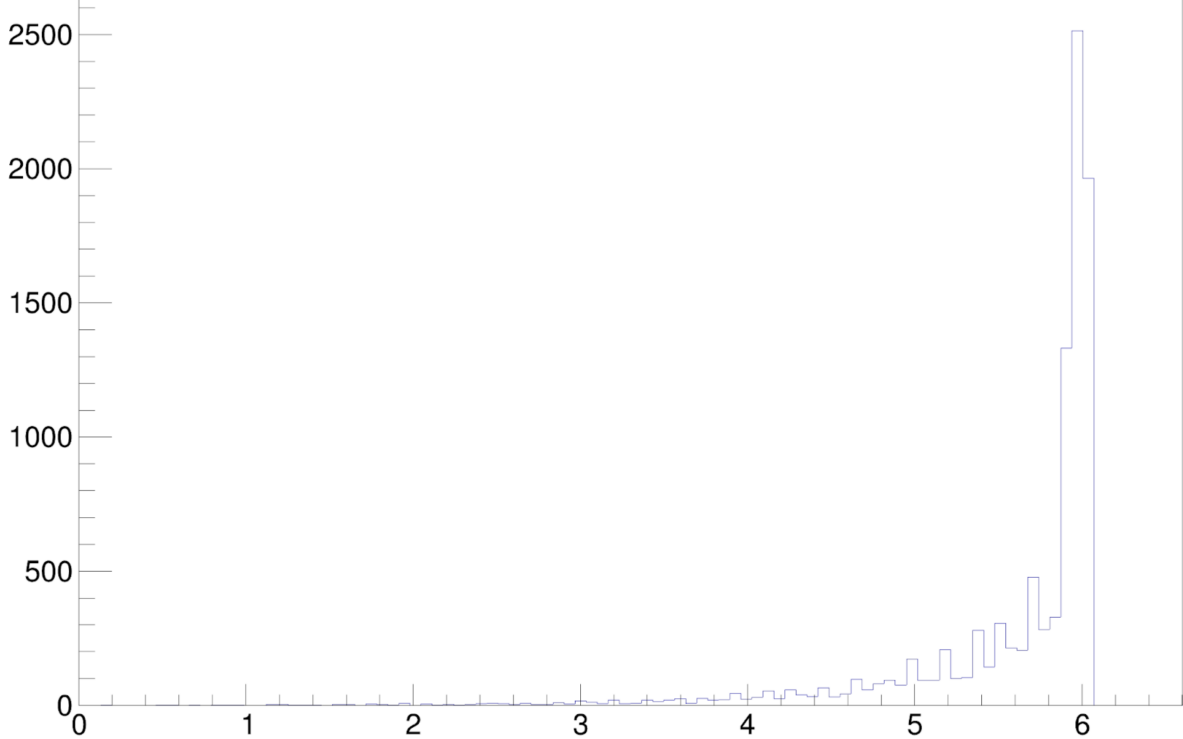


Figure 9: The distribution of weights in the simulation for the sample with neutrino interactions generated only within the decay volume held at atmospheric pressure.

for all generated neutrino interactions in the simulated sample, which is consistent with the expected value.

The results of applying the basic selection are shown in Table 4.

Conclusions and future plans. Different studies were performed to evaluate the neutrino-induced background for both experimental sites: ECN4 and ECN3. All studies show consistent behaviour. It was shown that for the default geometry we are able to obtain 0.2 muon neutrino-induced background events for the partially reconstructed events, even if we do not use the information from the surrounding tagger. If the geometry is changed to relax the vacuum requirement and use helium in the decay volume instead, the fully reconstructed signal candidates will get 0.2 additional muon-neutrino-induced background events. For the partially reconstructed signal events, only 0.3 additional muon-neutrino-induced background events are achievable if the information from the surrounding background tagger is also used. Studies were conducted to understand the potential of the experiment in background suppression. More complicated algorithms should be implemented, and the selection should also be tuned to the decay of multibody signals. This work is planned next:

- PID selection should be improved to account for multibody signal decays.
- Files with results of neutrino interactions on nuclei should be updated with GENIE v3.
- Studies are performed with muon neutrinos, whose fluxes dominate in the experiment. The contributions of the other neutrino flavours should be added.
- Advanced SBT algorithm using only partial information from the SBT should be integrated for selection.

		Expected in 5 years atmospheric pressure	Expected in 5 years helium
Fully reconstructed events (IP < 10 cm)	Basic selection	1.54	0.19
	Basic selection and SBT	1.18	0.15
Partially reconstructed events (IP < 250 cm)	Basic selection	110	14
	Basic selection and SBT	2.1	0.26

Table 4: The table shows the number of additional neutrino-induced events after selection from the decay volume with relaxed requirements. The simulation was performed with a decay volume kept at atmospheric pressure. The number for helium is given for estimation purposes only and was determined by dividing the number for atmospheric pressure by the density ratio.

- The selection cuts should be re-evaluated on the signal sample when the decay volume is kept at atmospheric pressure.
- The selection should be updated with digitised information from the upstream tagger.

2 Muon DIS

Maksym Ovchynnikov, Anupama Reghunath, Oliver Lantwin

Much like the neutrinos, studying the deep inelastic scattering (DIS) of muons is critical to ensure zero background in the SHiP detector. Muons interacting in the vessel wall could produce SM particles with decay signatures that closely resemble those of actual signal events. Therefore, understanding and characterizing these muon DIS backgrounds are essential steps in distinguishing genuine signal events from background noise in SHiP experiments.

There are two crucial differences between a muon-driven background and a neutrino-driven background. First, the muon DIS cross-section is much larger, which means that the total number of background events will be much larger. It makes it complicated to achieve the 1-to-1 correspondence between the simulated sample and the full amount of backgrounds to be observed during the 15-year running time of SHiP. Because of this, instead of calculating the expected background left after imposing selection and vetoing, we will obtain the statistical upper bound on the expected events.

Second, muons are charged and leave depositions in the walls of the decay volume. It may be used to veto the background by correlating the observed candidate events with the veto systems activity. On the other hand, it introduces challenges, such as false vetoing and dealing with differentiating between the background and the signal with wide angular distribution of decay products, which is typical for decaying new physics particles with mass $m \gtrsim 1$ GeV.

The SHiP LoI studies considered the decay volume filled by 1 mbar air. The study has several limitations:

- The current baseline material of the decay volume is helium at normal conditions ($\rho \simeq 1.7 \cdot 10^{-4}$ g/cm³).
- Lack of statistics: too few dangerous muons were simulated in the sample, too low ratio $N_{\mu \text{ DIS,sampled}}/N_{\mu \text{ DIS,expected}} \sim 10^{-4}$.
- Only a primitive SBT veto criterion has been used, which may result in falsely vetoed events with true signal.

To improve the study, a re-analysis is being performed. In short, it uses muons simulated per 10 spills (the LoI one uses 1-spill data), considers both the 1 mbar air (to cross-check the LoI study) and helium options, and simulates more DIS events per single muon.

2.1 Simulation details

Simulation of the muon background is done in two stages. The first stage is the more computationally intensive simulations of the target and the hadron absorber (HA). Since the target and HA are optimized as part of the BDF and not actively modified, their performances can be simulated separately within the FairShip framework. This process is referred to as pre-production. Only the particles that successfully pass through the (non-magnetized) HA are saved in the pre-production to be transported through the remainder of the experimental setup at the second stage.

The pre-production data is stored across 67 files, and is available in
`/eos/experiment(ship)/data/Mbias/background-prod-2018/`

Each muon in this sample is assigned a weight (w_{μ}) to account for the enhanced processes, such that the cumulative sum

$$\sum_{i=1}^{67} (\sum w_{\mu}) = N_{\mu}^{\text{spill}} = 1.80178 \cdot 10^{10},$$

where N_μ^{spill} is the number of muons exiting the HA per nominal SHiP spill.

To investigate muon DIS background effects, these files are reloaded and propagated throughout the entire experiment starting from the target. The propagation significantly depends on the configuration of the muon shield. They are generated using the fast muon option, i.e. only the muon hits are recorded.

For the SHiP LoI studies, the 1-spill weighted dataset has been generated. Following the muon shield suppression (Baseline configuration SC; superconducting option for the muon shield optimized for the ECN3 cavern), approximately $\mathcal{O}(10^5)$ unweighted muons remain in the dataset, which can be accessed from

```
/eos/experiment/ship/user/edursov/SC_full_opt_1/sc_v6_full_spill/sc_v6_merged.root
```

The studies described in this report also use the same baseline configuration SC, but a larger dataset is generated accounting for 10 spills:

```
/eos/experiment/ship/user/edursov/SC_full_opt_1/sc_v6_10_spills/sc_v6_MERGE.root
```

These muons are then analyzed separately depending on their trajectory:

- Muons hitting the entrance lid of the decay volume, and subsequently the tracking stations (“**front**”).
- Muons hitting only the decay vessel’s side walls (“**side**”).
- Muons hitting only the cavern (“**cavern**”).

The classification is useful since they contribute differently to the number of events. Namely, the events from cavern muons may be easily rejected by imposing the impact parameter cut on the candidate vertex. The events from **side** muons have a smaller impact parameter, typically belonging to the so-called partially reconstructed candidates.¹ Finally, the **front** muons would generate the events with the smallest impact parameter, corresponding to the fully reconstructed candidates.

2.2 front and side muons

This separation of the muons after passing the muon shield onto **front** and **side** ones is done using the `make_nTuple.py` script available in the repository, by passing the desired type as the argument. The resulting output `muons<type>.root` containing the subset of the muons is then processed for DIS production.

The numbers of muon entries for **front** and **side** muons are, correspondingly,

$n_{\text{front}} = 35$, $n_{\text{side}} = 6072$, for the 1-spill dataset and

$n_{\text{front}} = 392$, $n_{\text{side}} = 62010$, for the 10-spill dataset.

The analysis process involves several steps:

1. The first part of the simulation is to generate the muon DIS. Currently, it is done with the help of `pythia6` as launched using the script `makeMuonDIS.py`.² One takes the muon’s energy E_μ and 3-momentum \mathbf{p}_μ as an input, generates the scattering in the frame where the muon’s 4-momentum has the form $k^\mu = (E_\mu, 0, 0, |\mathbf{p}_\mu|)$, and then rotates to the frame defined by \mathbf{p}_μ . Note that the way `pythia6` generates the value of the cross-section is iterative: event-by-event, it converges from some random value $\sigma_{\text{DIS}}^i(E_\mu)$ being widely distributed around the “true” value to the final result $\sigma_{\text{DIS}}(E_\mu) = \lim_{i \rightarrow \infty} \sigma_{\text{DIS}}^i(E_\mu)$. To account for this issue and artificially extend the statistics, one generates many DIS events

¹The contribution of the DIS events from **side** muons to the fully reconstructed candidate events depends on the particular geometry and, in particular, on the angle of widening the decay volume.

²Replacement with `pythia8` is in progress.

$N_{\text{per muon}}$ per given muon. For all the generated events, one uses the converged DIS cross-section.

The LoI study operated with $N^{\text{front}} = 7000$ and $N^{\text{side}} = 700$, whereas the fast current study used involved $N^{\text{front}} = 10000$ and $N^{\text{side}} = 100$. This way, it provided comparable numbers of the entries for the `side` muons (but with improved diversity) and more than one order of magnitude larger amount of entries for front muons (see also the second column of Table 6).

2. The next part of the simulation is to distribute the DIS vertex of the muons according to the material budget. This part of the simulation is launched using the `FairShip` script `run_simScript.py` with the simulation engine "`muonDIS`".

The differential probability of scattering at a point belonging to some domain `domain` is

$$\left(\frac{dP_{\text{DIS}}}{dl} \right)_{\text{domain}} = \sigma_{\text{DIS}}(E_\mu) \cdot A \cdot n_{\text{domain}} = \sigma_{\text{DIS}}(E_\mu) \cdot N_A \cdot \rho_{\text{domain}}, \quad (1)$$

where l is the distance along the trajectory of the muon, A is the atomic number and n_{domain} the number density of the point. Examples of domains are the decay volume vessel, cavern wall, low-pressure gas inside the decay volume, etc.

Summing over all the materials, we get

$$P_{\text{DIS}} = \sum_{\text{domains}} \left(\frac{dP_{\text{DIS}}}{dl} \right)_{\text{domain}} l_{\text{domain}} \equiv \sigma_{\text{DIS}}(E_\mu) \cdot N_A \cdot \rho l \cdot \sum_{\text{domain}} \omega_{\text{domain}}, \quad (2)$$

with l_{domain} being the length of the trajectory belonging to the given domain,

$$\rho l \equiv \sum_{\text{domains}} (\rho l)_{\text{domain}} \quad (3)$$

the integrated density-times-path, while the weights $\omega_{\text{domain}} = (\rho l)_{\text{domain}} / \rho l$ define the relative probability for the DIS to occur inside the given domain.

Compared to the default run of `run_simScript.py`, two changes have been made. First, before participating in DIS, muons encounter a lot of soft interactions, such as ionization. These interactions would change its trajectory and energy, but not significantly. However, on the other hand, they are very important for vetoing such muons, so they cannot be neglected. To implement this in the simulation, together with the DIS products, one generates the fake muon with the energy $E_{\text{fake}} = E_\mu$ and the 3-momentum $\mathbf{p}_{\text{fake}} = -\mathbf{p}_\mu$, propagating in the opposite direction. Its soft interactions are enabled by switching `InactivateMuonProcesses` option to `False`. This choice is too wide – it allowed not-so-soft interactions such as proton bremsstrahlung. In the current simulation, the option is kept `True`, but with the removed string

```
mygMC.ProcessGeantCommand("/process/inactivate muIoni")
```

(This command turns off the muon ionization processes).

3. The events simulated by the previous script are then reconstructed using the `ShipReco.py` script.
 - Finally, the reconstructed events that do not pass the signal selection are filtered and saved. The selection cuts used here are shown in Table 5.

Cut	Value
Good daughters	$n_{\text{DoF}} > 25, \chi^2/n_{\text{DoF}} < 5, p_{\text{track}} > 1 \text{ GeV}$
Number of “good” candidates per event	1
DOCA	$< 1 \text{ cm}$
Vertex distance from vessel’s wall	$> 5 \text{ cm} (\text{transverse}), 20 \text{ cm} (\text{longitudinal})$
IP (f.r.)	$< 10 \text{ cm}$
IP (p.r.)	$< 250 \text{ cm}$

Table 5: Event selection criteria on the muon-DIS background.

Further background rejection is achieved using veto systems like the SBT and UBT. The SBT veto is triggered by any SBT activity per event with the energy deposit per SBT cell being $E_{\text{deposit}} > 45 \text{ MeV}$. All the launching commands and specifications for the simulation steps mentioned are available in a dedicated muonDIS README within the main **FairShip** repository.

We may relate the simulated sample to the expected events by the formula

$$N_{\text{DIS,expected}} = \sum_{i=\text{front,side}} N_{\text{DIS,expected}}^i, \quad (4)$$

where

$$N_{\text{DIS,expected}}^i = \frac{N_{\text{spills}}}{N_{\text{per muon}}^i} \sum_j \omega_{\mu}^{(j)} \cdot P_{\text{DIS}}^{(j)}, \quad (5)$$

where N_{spills} is the number of n -spills per 15-year running time of SHiP for which the fast muon simulation has been performed ($n = 1$ for the SHiP LoI study, $n = 10$ for the current studies), and the summation is done over the sampled ($n \times N$)_j events.

From the table, we see that the current analysis for the 1 mbar air option qualitatively reproduces the results of previous studies. Comparing the helium and air options, we find that the number of simulated samples for both the helium and vacuum options scales with the density of the decay volume $\rho_{\text{decay volume}}$, which serves as a cross-check. The trivial conclusion is there is a significant increase in the number of events passing all kinematic pre-selection cuts for the helium option compared to the vacuum option. For fully reconstructed events, the ratio of DIS events inside the decay volume to the total number of events was approximately 2.5% for helium and less than 0.01% for 1 mbar air.

The influence of helium on the DOCA distribution was also analyzed. For events with DIS vertices outside the decay volume, the DOCA was slightly larger in the helium case, likely due to rescattering off helium atoms. When including events with DIS vertices within the decay volume, the average DOCA decreased.

By imposing simple kinematic pre-selections and SBT, UBT vetoing, from the simulated sample in both the past and current studies $N_{\text{DIS,expected}} = 0$, see Table 6. But given that $N_{\mu \text{ DIS,sampled}} \ll N_{\mu \text{ DIS,expected}}$ for the events with at least 1 good candidate, a statistical estimate for the expected background is calculated using the weights. If after all cuts $N_{\mu \text{ DIS,sampled}} = 0$, a 90% CL upper limit on the rejection efficiency is imposed. The main assumption here is that the veto cuts and the kinematic cuts are statistically independent. Details may be found in the PhD thesis [3], p. 82.

For illustration, consider the LoI study. The expected number of DIS events with one good candidate is

$$N_{\text{DIS,expected}}^{\text{vtx}} = N_{\mu \text{ DIS,expected}} \cdot \epsilon_{\text{vtx}} \quad (6)$$

Setup	Details	$N_{\text{DIS}}^{\text{vtx}}$	$N_{\text{DIS}}^{+\text{Fid. vol.}}$	$N_{\text{DIS}}^{+\text{DOCA}}$	$N_{\text{DIS}}^{+\text{IP250}}$	$N_{\text{DIS}}^{+\text{IP10}}$
LoI	1-spill μ data 1 mbar air $(n \cdot N)_{\text{side}}: 4.3 \cdot 10^6$ $(n \cdot N)_{\text{front}}: 2.5 \cdot 10^5$	$2.2 \cdot 10^8$	$5.7 \cdot 10^7$	$5.1 \cdot 10^6$	$2.8 \cdot 10^5$	$7.1 \cdot 10^3$
2024_{vac}	10-spill μ data 1 mbar air $(n \cdot N)_{\text{side}}: 6.2 \cdot 10^6$ $(n \cdot N)_{\text{front}}: 3.9 \cdot 10^6$	$3.5 \cdot 10^8$	$6.2 \cdot 10^7$	$5.5 \cdot 10^6$	$1.9 \cdot 10^5$	$1.3 \cdot 10^3$
2024_{He}	10-spill μ data He (20°) $(n \cdot N)_{\text{side}}: 6.2 \cdot 10^6$ $(n \cdot N)_{\text{front}}: 3.9 \cdot 10^6$	$3.5 \cdot 10^8$	$6.5 \cdot 10^7$	$5.9 \cdot 10^6$	$4 \cdot 10^5$	$8.1 \cdot 10^3$

Table 6: DIS events per full SHiP timeline of 15 years (corresponding to $N_{\text{PoT}} = 6 \times 10^{20}$); effect of subsequent application of cuts. The meaning of the columns is as follows: the setup, its brief description, the number of muon DIS events with exactly one candidate, the number of events additionally passed the fiducial cuts (the vertex inside the decay volume, displaced from its walls), additionally passed the DOCA cut, the impact parameter cut for partially reconstructed candidates ($\text{IP} < 2.5 \text{ m}$), the impact parameter cut for fully reconstructed candidates ($\text{IP} < 10 \text{ cm}$). The setup corresponds to the SHiP LoI study, whereas the two 2024 setups describe the fast recent studies performed for the 1 bar air and helium materials of the decay volume (see the rest of the section for details).

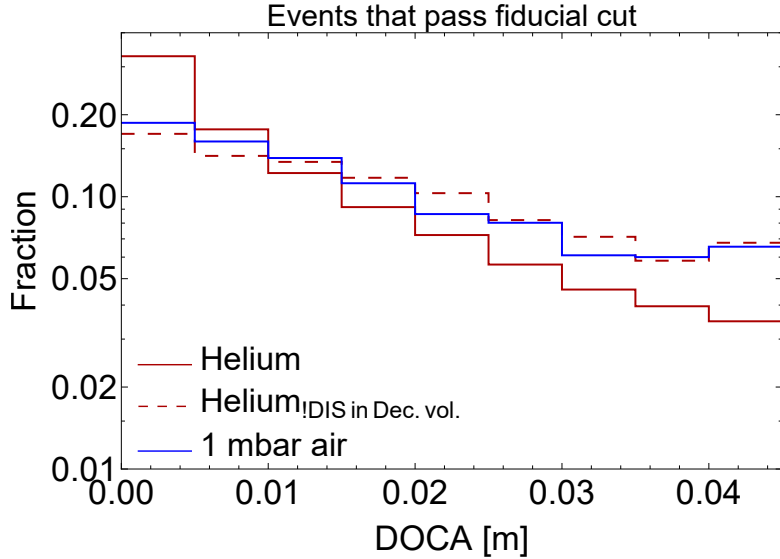


Figure 10: influence of helium environment inside the decay volume in DOCA distribution. The contribution of DIS events occurring inside the decay volume results in a peak at small DOCA values compared to the air option. If such events are removed, the distribution will shift slightly to large DOCA values, which is expected due to rescattering of the products off helium.

Setup	$N_{\text{DIS}}^{\text{pre-sel}}$	$N_{\text{DIS}}^{\text{pre-sel+SBT}}$	$N_{\text{DIS}}^{\text{pre-sel+SBT+UBT}}$
2024_{vac}	$1.9 \cdot 10^5$	73	0
2024_{He}	$4 \cdot 10^5$	718	0

Table 7: DIS events per full timeline; effect of veto.

Setup	$N_{\text{DIS}}^{\text{pre-sel}}$	$N_{\text{DIS}}^{\text{pre-sel+SBT}}$	$N_{\text{DIS}}^{\text{pre-sel+SBT+UBT}}$
2024_{vac}	$1.9 \cdot 10^5$	73	0
2024_{He}	$4 \cdot 10^5$	718	0

Table 8: DIS events per full timeline; effect of veto

where $\epsilon_{\text{vtx}} = 8 \cdot 10^{-3}$ is the efficiency of selecting the events. The 90%CL upper limit is then

$$\text{UL(90% CL)} = -\ln(0.1) \frac{N_A \langle \rho \cdot l \rangle \langle \sigma_{\text{DIS}} \rangle}{\chi}, \quad (7)$$

where

$$\chi = N_{\mu \text{ DIS}}^{\text{samples,vtx}} / N_{\mu \text{ DIS}}^{\text{vtx}} \quad (8)$$

is the scaling between the simulated samples and Eq. (5), and $\langle \dots \rangle$ as usual denotes the expectation value, estimated using the sample average. Explicitly, we have $N_{\mu \text{ DIS}}^{\text{vtx}} = 2.2 \cdot 10^8$, $N_{\mu \text{ DIS,sampled}} = 5.9 \cdot 10^4$, and $N_A \langle \rho l \rangle \cdot \langle \sigma_{\text{DIS}} \rangle = 1.8 \cdot 10^{-2}$. Therefore,

$$\text{UL(90% CL)} = 166 \quad (9)$$

Therefore, the veto inefficiency is

$$\epsilon_{\text{veto}} < \frac{\text{UL(90% CL)}}{N_{\text{DIS}}^{\text{vtx}}} < 8 \cdot 10^{-7} \quad (10)$$

it gives us the statistical upper bound on the expected number of DIS events:

$$N_{\text{DIS}}^{\text{...+IP250+veto}} < 0.2, \quad N_{\text{DIS}}^{\text{...+IP10+veto}} < 5.6 \cdot 10^{-3} \quad (11)$$

Similar bounds hold for the ongoing study.

By accumulating more statistics, they may be lowered even more.

Overall, the number of DIS events at various stages of selection for different setups shows a substantial difference between vacuum and helium options. For the 2024 vacuum setup, there were 1.9×10^5 DIS events passing pre-selection, reduced to 73 after the SBT, and to zero after the UBT. For the 2024 helium setup, the numbers were 4×10^5 , 718, and zero, respectively. The contribution of events with DIS inside the decay volume, after imposing SBT, was 85.6% for helium and approximately 1.4% for 1 mbar air. These results also highlight the need for further investigation into the effects of veto systems and improved signal-background discrimination techniques.

Most events analyzed had low-multiplicity DIS vertices, see Fig. 11. An example of a low-multiplicity DIS event is given by the reaction $\mu + Z \rightarrow Z' + n + \mu + 2\pi$, where Z' is at rest, n is very soft, and the $\mu\pi\pi$ system forms a candidate that cannot be vetoed with the SBT. Such events can be discriminated by requiring a zero total electric charge of all daughter particles that are reconstructed. However, events with higher multiplicity also play a crucial role.

As an example from the study, one event with six DIS products had only one product fly to the side walls, which was a soft neutron with $E_k \approx 60$ MeV, insufficient to leave a significant deposit in the SBT. Another event with six DIS products had none of the products fly to the side walls. To improve upon this veto, further studies fully exploiting the information from the SBT/UBT to produce a more advanced vetoing are being done in parallel.

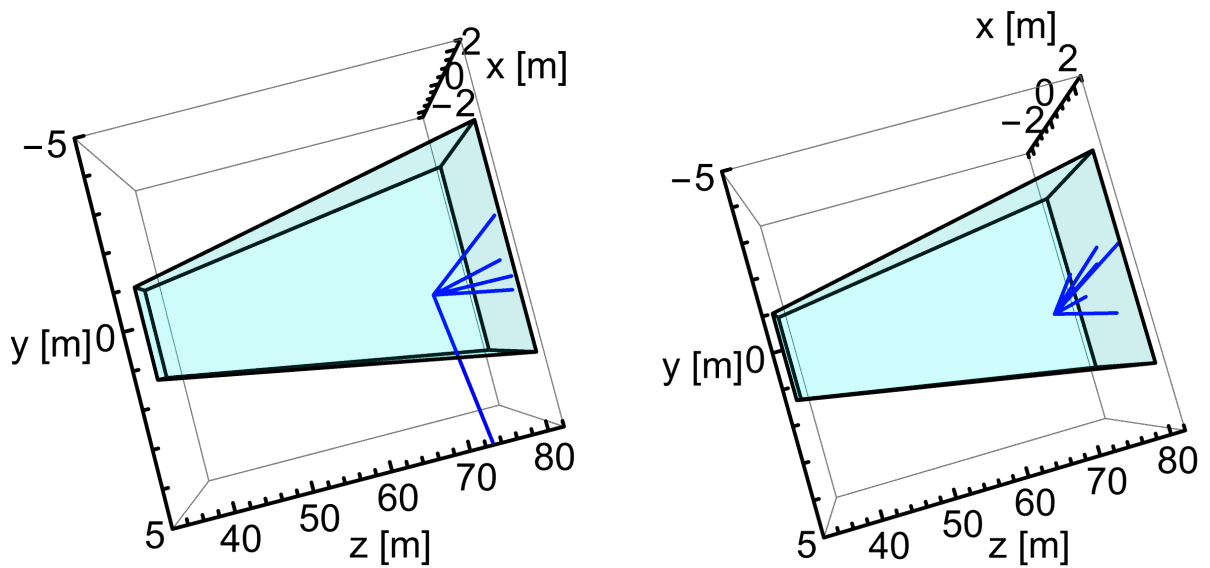


Figure 11: Example DIS events that cannot be vetoed with the current SBT criterion.

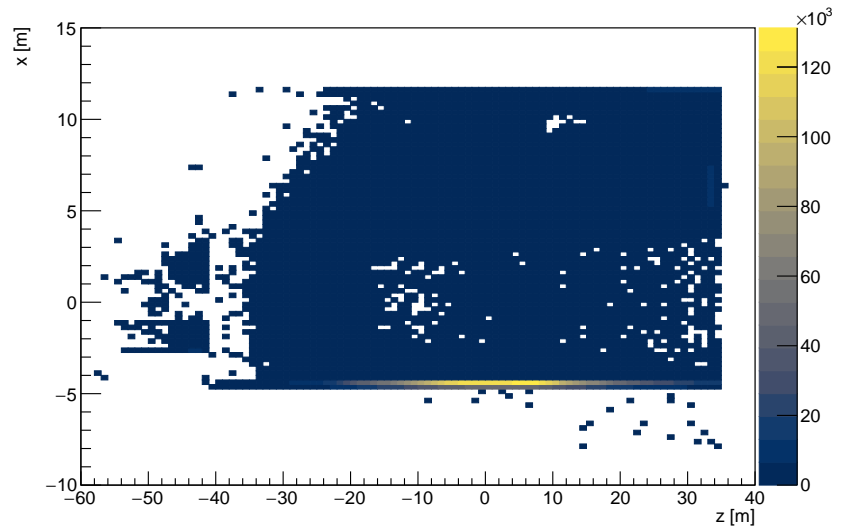


Figure 12: Impact point of muons in the cavern in the bending plane of the muon shield.

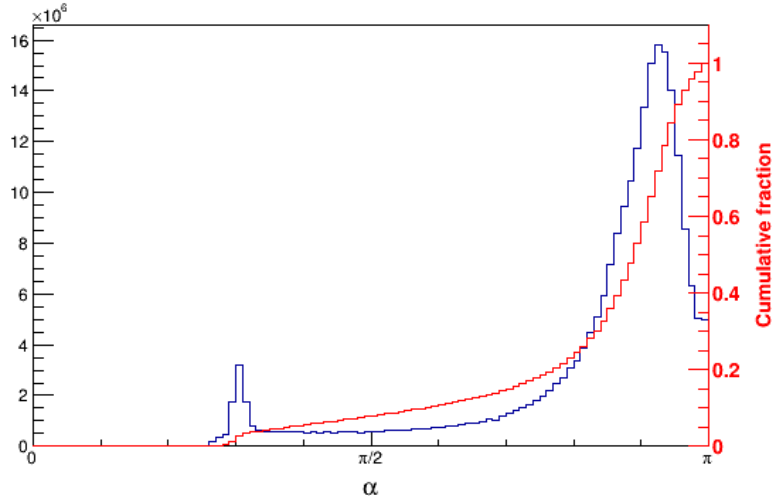


Figure 13: Distribution and cumulative distribution of the muon direction and the decay vessel.

2.3 Cavern muons

Oliver Lantwin

Due to the experimental geometry, it is not expected that deep-inelastic scattering of muons in the cavern walls will produce a non-negligible background. To confirm this intuition, a worst-case estimate assuming factorisation has been performed for both ECN4 and ECN3, and is presented in following. For a description of an earlier study for ECN4, please see Ref. [3]. For the ECN3 location the most important change is the reduced distance of the decay volume from the cavern walls on the Salève side of the experiment, which results in the muons impacting the cavern walls further upstream, shown in Fig. 12, increasing the potential acceptance for muon DIS products in the decay vessel. Despite this more favourable impact point, the angles that decay products would require to reach the decay volume are large, as can be seen in Fig. 13.

As the interaction products from muon DIS tend to follow the muon direction, only a negligible fraction of them show these large angles and none of the DIS events studied have lifetimes long enough or momenta high enough to create V^0 type events in the decay vessel. Assuming for a moment that some did, the particles point upstream, not downstream, so that at least a three-body decay is required to pass even the loosest pre-selection. Again, the kinematics prove prohibitive, with the phasespace of candidate three-body decays with sufficiently extreme angles being negligible. Adding potential other activity that could be tagged using the SBT, and the loose pre-selection for partially reconstructed signal candidates, backgrounds from DIS interactions in the cavern walls appear very implausible.

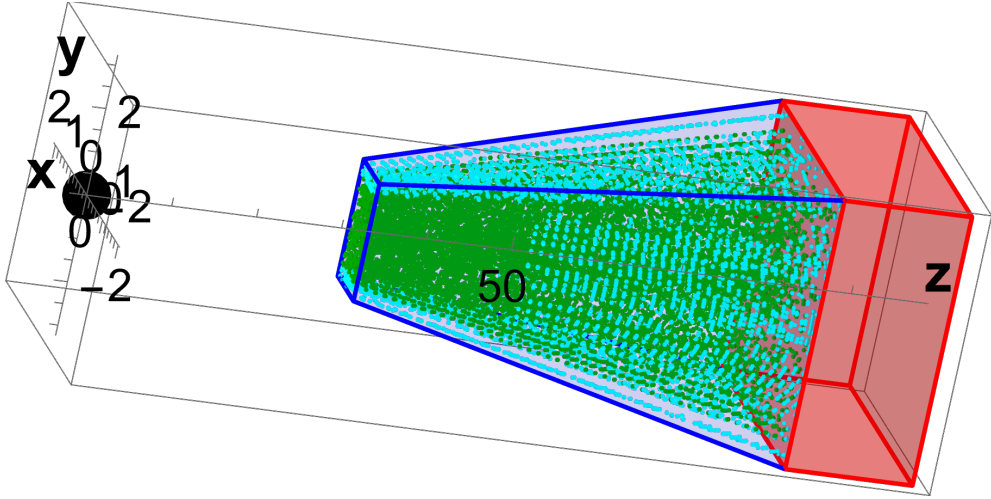


Figure 14: Geometry of the SHiP experiment as implemented with the SHiP-ECN3 setup in `SensCalc`. The blue domain shows the decay volume, while the red domain indicates the detector. The points show the grid in θ, z, ϕ used to calculate the map of decay products acceptances.

3 Sensitivities to feebly-interacting particles

Maksym Ovchynnikov

To compute the sensitivity curves for various models with long-lived particles (LLPs)³ as shown in Fig. 50 of [4], the `Mathematica`-based tool `SensCalc` [5] has been used. It is based on the semi-analytic approach to calculate the number of events as described in Ref. [6]. The main purpose of `SensCalc` is to have a public, transparent, and robust way to estimate the sensitivity curves, yet simplified compared to the full simulation.

The current version does not include the detector reconstruction effects, which, in particular, leads to the perfect 4-momentum reconstruction, etc., and hence to the unit reconstruction efficiency. The latter is expected to be $\mathcal{O}(1)$ for the events that pass the baseline event selection criterion.⁴ Therefore, its effect would not be visible in the logarithmic plots with the parameter space of new physics particles.

The generic usage of `SensCalc` is described in the .pdf readme file stored in the cited repository. In short, it is enough to launch the notebooks and pass through the set of dialog windows asking for the various inputs.

The implemented models with LLPs correspond to: *DP* — BC1, *Scalar* — BC4-5, *HNL* — BC6-8 (*HNL-mixing-e* — BC6, *HNL-mixing-mu* — BC7, *HNL-mixing-tau* — BC8, and arbitrary mixing pattern is also possible), *ALP-photon* — BC9, *ALP-fermion* — BC10, *ALP-gluon* — BC11.

In the notebook **1. Acceptances.nb**, that produces the tabulated geometric and decay products acceptance, one must select SHiP-ECN3 for the experiment. It corresponds to the geometry of the decay vessel and detector currently implemented in `FairShip`. Fig. 14 shows a schematic geometry of the setup.

Then, one must specify the following selection cuts:

- $\{\{1, -999\}, \{1, -999\}, \{1, -999\}\}$ for the minimal/maximal energy of the detectable

³Equivalently, feebly-interacting particles, or FIPs.

⁴See [Iaroslava's talk](#) on the neutrino DIS events, where she also discussed the reconstruction efficiency for the signal by considering a few decay modes of heavy neutral leptons.

charged particles.

- $\{\{1, -999\}, \{1, -999\}\}$ for the minimal/maximal energies of the detectable neutral particles.
- 2.5 for the transverse impact parameter cut.

The rest of the parameters must be kept at their default values.⁵

At the stage of selecting the given model with an LLP, the default options must be chosen. They correspond to considering the decay modes with at least two charged particles with zero total charge as potentially detectable and hadronizing partonic decay products in `pythia8`. Other choices are possible; for instance, one may be required to detect at least n particles, which is important for fully reconstructible events. For the BC10 case, in addition, the phenomenology choice *New* must be made.

The notebook then evaluates the azimuthal acceptance $\epsilon_{\text{az}}(\theta, z)$, which shows the fraction of the azimuthal coverage $-\pi < \phi < \pi$ for which the given point θ, z is inside the decay volume, and the map of the decay products acceptance for the given LLP. Let us briefly describe the latter. Consider a LLP with mass m and energy E , decaying at the point parametrized by the polar angle θ , the longitudinal displacement z , and the azimuthal angle ϕ . The notebook then calculates a fraction of decay events for which at least two of the decay products point to the end of the detector and satisfy the other cuts, $\epsilon_{\text{dec}}(m_{\text{LLP}}, \theta, E, z) \leq 1$. This is done in the following way: First, the phase space of various LLP decays is calculated;⁶ Second, for the grid of θ, E, z and associated azimuthal angles $\{\phi\}$ inside the decay volume, it calculates the fraction of decay events that pass the selection criteria. Finally, it averages over the values of ϕ (as ϕ s do not enter any other quantity determining the number of events), to get the tabulated grid $\{m, \theta, E, z, \epsilon_{\text{dec}}\}$. More details are given in Ref. [6]. The effect of the magnetic field is implemented as a kick accumulated when passing the region in a homogeneous magnetic field.

In the notebook **2. LLP distribution**, which produces tabulated angle-energy distributions $f_{\text{LLP}}^{(i)}(\theta, E)$ for different production channels $\{i\}$ with LLPs, one has to select “SPS” for the facility, and then generate the distributions for all the proposed production channels (the option *All channels*) for the given LLP. For the number of simulated events where a Standard Model particle decays into LLPs, one should choose $10^6 - 10^7$. To calculate the distribution from n -body decays with $n > 2$, the notebook takes the squared matrix elements of the processes and samples the true kinematics.

Examples of the angle-energy distributions for some production modes are shown in Fig. 15.

Finally, the notebook **3. <LLP> sensitivity.nb** computes the tabulated number of events as a function of the LLP’s mass and coupling to the Standard Model. It is done by using the following integral:

$$N_{\text{events}} = N_{\text{PoT}} \cdot \sum_i P_{\text{prod}}^{(i)} \int dz d\theta dE f_{\text{LLP}}^{(i)}(\theta, E) \cdot \epsilon_{\text{az}}(\theta, z) \cdot \frac{dP_{\text{decay}}}{dz} \cdot \epsilon_{\text{dec}}(\theta, E, z), \quad (12)$$

where $P_{\text{prod}}^{(i)}$ is the production probability of the LLP, and $\frac{dP_{\text{decay}}}{dz}$ is the differential decay probability:

$$\frac{dP_{\text{decay}}}{dz} = \frac{\exp[-z/(\cos(\theta)c\tau\sqrt{\gamma^2 - 1})]}{c\tau\sqrt{\gamma^2 - 1}}, \quad (13)$$

⁵The rest of the selection cuts specified in [4] is by definition satisfied in the current version of `SensCalc`.

⁶Evaluating it at the rest frame of the decaying LLP and then boosting it to the laboratory frame defined by the LLP energy and angles θ, ϕ). for decays into 3 and more decay products, the squared matrix element in terms of energies E_1, E_3 of the decay products 1,3 is used.

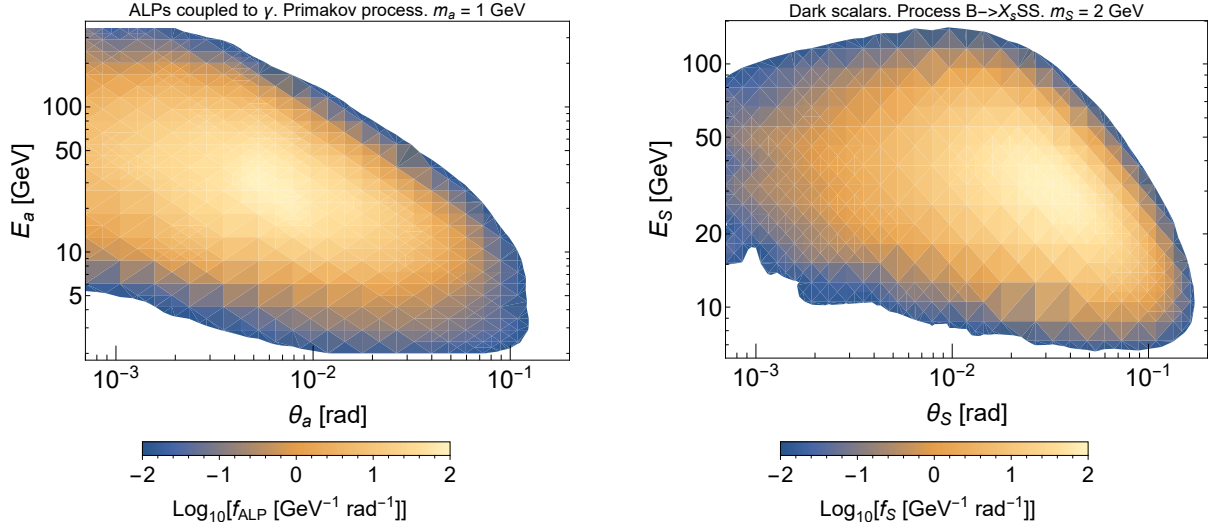


Figure 15: Examples of angle-energy distributions $f^{(i)}(\theta, E) \equiv d^2 f_{i \rightarrow \text{LLP}} / d\theta_{\text{LLP}} dE_{\text{LLP}}$ for ALPs coupled to photons (**left**) and dark scalars with a non-zero quartic coupling (**right**), produced by the notebook `FIP distribution.nb` for the SHiP beam-target configuration.

with $c\tau = c\tau(m, g)$ being the proper lifetime of the LLP with the coupling g to the Standard Model.

One should select the option *Tabulated Nevents + sensitivity* at the very beginning,⁷ then select **SHiP-ECN3** at the stage when the experiment is chosen, wait until the tabulated number of events is computed, and then produce sensitivities. At the stage of producing the sensitivities, one should select the model (in case of some non-minimal parameters and/or various phenomenology description choices), and then proceed with the default set of parameters (the number of protons on target, the minimal detectable number of events, the production channels) to compute the sensitivity curve.

Depending on the LLP, non-minimal selection is needed:

- For HNLs: the mixing pattern $\{U_e^2, U_\mu^2, U_\tau^2\}$ and type – Dirac or Majorana. The Majorana type and the patterns $\{1, 0, 0\}$, $\{1, 0, 0\}$, $\{0, 0, 1\}$ correspond to the BC6, BC7, BC8 models.
- For Higgs-like scalars: the choice of the branching ratio $\text{Br}(h \rightarrow SS)$ defines the model. The zeroth value corresponds to BC4, while 0.01 means BC5. Also, for the description of the production from B mesons, *Exclusive* must be chosen.
- For ALPs coupled to fermions: the *Revised* phenomenology must be used.

Some intermediate useful plots may be produced during the run of the notebook, see Fig. 16.

Finally, the notebook **4. Plots** produces plots with the sensitivities. Just navigate to the section with the given LLP, and launch it.

⁷Once the tabulated number of events is produced for the given model input/experiment and one just wants to compute the sensitivity assuming different parameters, one should choose the option *Sensitivity only (tabulated Nevents must be produced before)*.

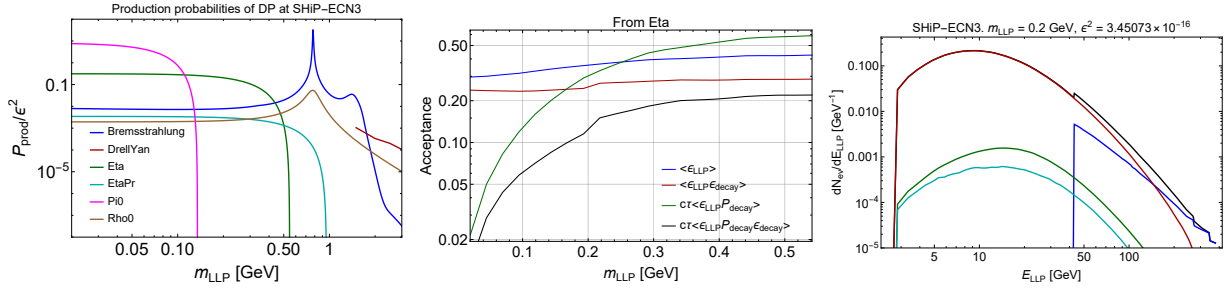


Figure 16: Examples of the auxiliary plots produced by the notebook 3. **DP sensitivity** that calculates the number of events with dark photons for the SHiP experiment. **Left:** The production probabilities (amount of produced dark photons per proton-on-target) from various channels normalized by the squared mixing angle ϵ^2 . **Middle:** various acceptances defining the position of the lower bound of the SHiP sensitivity (i.e., when $c\tau\langle\gamma\rangle \gg 100$ m) for the dark photons produced by decays $\eta \rightarrow \gamma + \text{DP}$ (see [6] for details). **Right:** the energy distribution of the dark photons for the decay events that pass the SHiP selection.

3.1 Future plans

Maksym Ovchynnikov, Martina Ferrillo, and Josue Jaramillo are developing the LLP event sampler `EventCalc`.⁸ It is a module that takes the tabulated angle-energy distribution of LLPs produced by `SensCalc` as well as the information about the production and decay probabilities of LLPs and produces the traditional event data in the form of information about decaying LLPs.

The event sampler will first take the LLP name, set of masses, and couplings for which the events have to be simulated. Then, it will ask about the LLP production and decay modes to be used for the simulation. This also includes the variation of the production and decay fluxes within their theoretical uncertainty bands, which may range by a few orders of magnitude depending on the LLP and dominate all the other uncertainties.

Once this is fixed, the sampler generates the kinematics of the produced LLPs within the SHiP decay volume, the position of the decay vertex, and decays for each of the LLPs. The information about LLP's mass and couplings gives the lifetime, which, together with the kinematics information, is then used to calculate the decay probability for each of the decayed LLPs. Their detailed description will be published elsewhere.

Details of the approach will be published in a dedicated paper (see also [7]).

The `Mathematica` version is finished, while the `python` version is being updated by adding new LLPs and implementing 4-body decays. The current activities are split into two topics that may be done in parallel. The first one is interfacing the output tables containing the information about the LLP and its decay products, and/or the `python` module itself to `FairShip`. The second one is cross-checking the calculations of the `python` version with `SensCalc` and `Mathematica`-based `EventCalc`.

`EventCalc` will provide a flexible framework to simulate the reconstruction of events with LLPs, which will be used not only to study the effects of finite detector reconstruction resolution on the events acceptance, but also to investigate the capabilities of SHiP to differentiate between the signal and background without using veto systems. It will allow us to test the performance of the setup depending on its parameters, such as the material and thickness of the decay vessel's walls, the quality of the veto system, and others. This way, it will improve both the background and signal studies.

⁸The `Mathematica` version may be found on [Zenodo](#) and [GitHub](#). The `python` version may be found on [GitHub](#).

The strategy is to generate events with various LLPs having different masses and lifetimes, to cover as many scenarios as possible:

- Decay products type – leptons, photons, or hadrons.
- Topology of the decays: whether they are two-body, or most of them are multi-body (high-multiplicity exclusive decays or decays into jets).
- Distribution of LLP’s decay vertices – isotropically inside the decay volume (if $c\tau_{\text{LLP}}\langle\gamma\rangle \gg 100$ m or concentrated at its entrance (the opposite regime)
- The width of the angular distribution of LLPs – limited to small angles $\theta \lesssim 0.01$ rad (such as the case of the proton bremsstrahlung or the Primakov process) or more isotropic (such as decays of B mesons).

Then, these events will be passed to a GNN trained on the muon and neutrino backgrounds, in order to check how well it may distinguish between signal and background events.

4 Muon combinatorial

Alex Marshall, Oliver Lantwin, Konstantinos Petridis

For a description of the muon combinatorial studies for the ECN4 setup, please see Refs. [3, 8].

A future version of this note will include further details for ECN3, but qualitatively and quantitatively the results are similar.

A Appendix

References

- [1] **SHiP** Collaboration, T. Ruf and H. Dijkstra, *Heavy Flavour Cascade Production in a Beam Dump*, .
- [2] **SHiP** Collaboration, T. Ruf and E. Van Herwijnen, *Description of the SHiP FixedTargetGenerator*, .
- [3] O. J. I. Lantwin, *Optimisation of the SHiP experimental design*. PhD thesis, Imperial Coll., London, 2019.
- [4] **SHiP** Collaboration, R. e. a. Albanese, *BDF/SHiP at the ECN3 high-intensity beam facility*, tech. rep., CERN, Geneva, 2023.
- [5] M. Ovchynnikov, *SensCalc*, Mar., 2024.
- [6] M. Ovchynnikov, J.-L. Tastet, O. Mikulenko, and K. Bondarenko, *Sensitivities to feebly interacting particles: Public and unified calculations*, *Phys. Rev. D* **108** (2023), no. 7 075028, [[arXiv:2305.13383](https://arxiv.org/abs/2305.13383)].
- [7] Y. Kyselov and M. Ovchynnikov, *Searches for long-lived dark photons at proton accelerator experiments*, [arXiv:2409.11096](https://arxiv.org/abs/2409.11096).
- [8] A. Marshall, *Machine learning based background simulations and R-parity violating neutralinos at SHiP and contributions to the angular analysis of $B^0 \rightarrow K^{*0}(\rightarrow K^+\pi^-)\mu^+\mu^-$ at LHCb*. PhD thesis, Bristol U., 2021.